

# Design and analysis pertaining to the aerodynamic and stability characteristics of a hybrid wing-body cargo aircraft

Ishaan PRAKASH<sup>\*1</sup>, Prithwish MUKHERJEE<sup>1</sup>, Ravichandrakumar KB<sup>1,a</sup>

\*Corresponding author

<sup>\*1</sup>Department of Aerospace Engineering, SRM University,  
Kattankulathur, Tamil Nadu 603203, India,  
i.shaan1594@gmail.com\*, mukherjee.prithwish05@gmail.com,  
ravichandrakumar.m@ktr.srmuniv.ac.in

DOI: 10.13111/2066-8201.2017.9.3.6

Received: 18 July 2017/ Accepted: 23 August 2017/ Published: September 2017

Copyright©2017. Published by INCAS. This is an “open access” article under the CC BY-NC-ND license (<http://creativecommons.org/licenses/by-nc-nd/4.0/>)

**Abstract:** Recent trends in aircraft design research have resulted in development of many unconventional configurations mostly aimed at improving aerodynamic efficiency. The blended wing body (BWB) is one such configuration that holds potential in this regard. In its current form the BWB although promises a better lift to drag (L/D) ratio it is still not able to function to its maximum capability due to design modifications such as twist and reflexed airfoils to overcome stability problems in the absence of a tail. This work aims to maximize the impact of a BWB. A design approach of morphing the BWB with a conventional aft fuselage is proposed. Such a configuration intends to impart full freedom to the main wing and the blended forward fuselage to contribute in lift production while the conventional tail makes up for stability. The aft fuselage, meanwhile, also ensures that the aircraft is compatible with current loading and airdrop operations. This paper is the culmination of obtained models results and inferences from the first phase of the project wherein development of aerodynamic design and analysis methodologies and mission specific optimization have been undertaken.

**Key Words:** Cargo Aircraft, Blended Wing Body, Hybrid Wing Body, Aircraft Design, Fuselage

## 1. INTRODUCTION

Energy is fast becoming a critical constraint on operations so much so it could reshape aircraft design in the near future. For cargo aircrafts which consume much of the aviation fuel each year only near-term solutions such as formation flying, winglets and other drag-reduction devices exist which do not provide the scale of savings sought in the long term. Hence dramatic changes in aircraft design are required to achieve significant reductions in fuel consumption. Previous work on design and analysis of blended wing body configurations show remarkable improvements in aerodynamic efficiency [1]. The performance improvement of Boeing BWBs over conventional subsonic transports based on equivalent technology has increased beyond the predictions of the early NASA-sponsored studies [2]. The following characteristics of the blended wing body design support its potential for the next generation cargo mobility fleet:

---

<sup>a</sup> Professor (O.G)

- Higher L/D ratio: Considerably lower drag penalty due to reduction in total aerodynamic wetted area.
- Higher lifting capacity: for the same wing span and fuselage length of a conventional cylindrical fuselage aircraft the BWB offers higher volume for payload.
- Option for distributed Propulsion: the unique design provides space to incorporate distributed turbo-electric propulsion [3].

The current work is an extension utilizing inferences of previous studies on blended wing body design. Despite these notable advantages the BWB poses several challenges:

- Stability: the BWB is an inherently unstable design. Several design parameters such as wing twist, sweep and reflexed airfoils are used to overcome the stability problems which ultimately lead to a reduced coefficient of lift. This is the cost paid for achieving required static stability margin. It is therefore very difficult to utilize the full potential of the BWB design in its current form [4].
- Compatibility: military and cargo operations are compatible with a cylindrical fuselage which has been one of the reasons for the success of this configuration. The BWB however does not offer this as the fuselage narrows toward the trailing edge. It is therefore not as flexible as the conventional design in terms of ease of loading and unloading cargo [5].

In order to utilize the full capacity of the BWB and ensure compatibility the proposed hybrid wing design incorporates a further blend with the conventional cylindrical fuselage. Further this allows for integrating cargo and cabin compartment with better flexibility such as the dual PAX pressurized cabin with rear and lateral cargo decks [6].

## 2. DEVELOPMENT OF DESIGN METHODOLOGY

Due to the unconventional nature of the configuration standard empirical estimation methods tend to increase errors and produce unrealistic results. A modified approach is hence developed incorporating class-II estimation methods to obtain realistic parameters and reduce estimation error. First a pure BWB design is developed with the objective of demonstrating its superior characteristics compared to a similar real world aircraft. After a baseline design is achieved modifications to address the stated issues is initiated. The developed methodology is shown in Fig. 1.

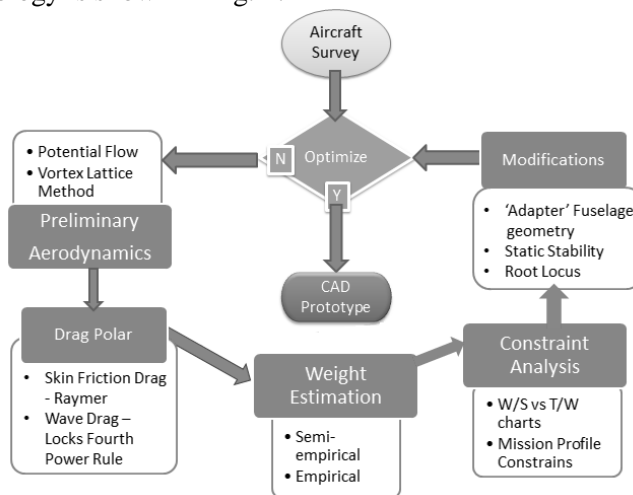


Fig. 1 – Design methodology schematic

The design process can be summarised in three primary phases. In the first phase from a cargo aircraft survey important design and performance parameters are fixed in order to begin the design iterations. Simultaneously geometric parameterisation of the design and development of robust preliminary aerodynamic modules is done to achieve a “baseline-1” design. In the second phase a combination of several empirical and semi-empirical techniques are used to develop a weight estimation algorithm. Further a constraint analysis algorithm subject to different flight profiles is developed and run giving the pure BWB “baseline-2”. In the third phase modifications in the geometry is done to morph the proposed adapter fuselage with the trailing edge of the “baseline-2”. After re-running previous algorithms a stability analysis module is developed to design the needed empennage. Finally using the parameters obtained for the “baseline-3” a CAD rendering is developed for future prototyping and CFD validation.

## 2.1 Preliminary Aerodynamics & geometric parameterisation

After a survey of several cargo aircrafts the C-17 Globemaster is chosen to initially fix parameters to begin the design process. Wing area, maximum take-off weight, payload weight and fuselage volume of the C-17 is taken for the baseline-1 BWB design [7]. To parameterise the geometry the body is divided into airfoil segments. Each segment can be defined using the following parameters as shown in Fig. 2: wing sweep, leading edge location, chord length and segment span.

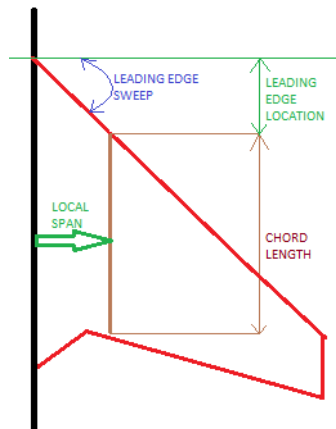


Fig. 2 – Parameterization

The payload volume of the C-17 is used to fix a root chord for the BWB. The aircraft is divided into the inner section and outer section. The inner section houses the payload volume and is hence constituted by high thickness airfoils. The outer section is designed as a typical swept back wing. Wing sweep is set by using the fixed cruise Mach number and wing span is set using the aspect ratio formula. Similar to the C-17 supercritical airfoils are chosen and a cruise Mach number of 0.75 is fixed. In order to obtain elliptic distribution it is required for mid-section  $C_l$  to be less as chord length is high. Hence reflex airfoils at mid length could serve the purpose and also possibly aid stability. Also the cabin angle constraints ( $<3$  degrees) conforms to this approach. In order to achieve a favorable design following four geometries of airfoil stack combinations from root to tip are loaded as AVL input files [8] and studied for span wise lift distribution:

1. Thick-supercritical-reflex
2. Reflex-Supercritical
3. Thick-reflex-Supercritical
4. Supercritical-Reflex

From basic potential flow and vortex lattice method analysis the third airfoil stack combination of reflex to supercritical gives the best possible lift distribution as seen in Fig. 3. In order to obtain a good lift distribution geometric twist is incorporated in each of the four combinations.

The wing is iterated to achieve a near elliptic distribution subject to cabin dimensions and angle constraints [9].

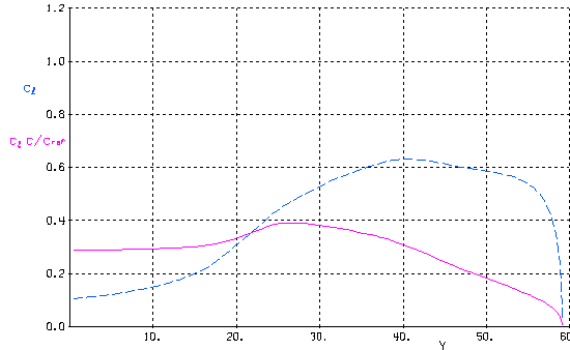


Fig. 3 – Half span lift distribution

## 2.2 Drag Polar: Compensating for skin friction and wave drag

In order to deduce the drag coefficients a module is developed which takes into account the induced drag, skin friction drag and wave drag. Essentially the induced drag is computed from the vortex lattice method, the skin friction drag is computed by logarithmic fit of Von Karman and the power law.

$$C_f = \frac{0.455}{\log(Re)^{2.58}} \quad (1)$$

Compressibility effect is added and finally a polynomial is fit using the least squares method to deduce the coefficients which would be required for the further constraint analysis. The obtained drag polar is shown in Fig. 4.

$$C_D = C_{D\ min} + K' C_L^2 + K'' (C_L - C_{L\ min})^2 \quad (2)$$

$K' \rightarrow$  Induced Drag

$K'' \rightarrow$  skin friction and pressure drag

Hence we get the polynomial,

$$C_D = K_1 C_L^2 + K_2 C_L + C_{D0} \quad (3)$$

$$K_1 = K' + K'' \quad (4)$$

$$K_2 = -2K'' C_{L\ min} \quad (5)$$

$$C_{D0} = C_{D\ min} + K'' C_{L\ min}^2 \quad (6)$$

The wave drag is estimated using Lock's fourth power rule which uses the critical Mach number computed by the following equations:

$$M_{crit} = M_{dd} - 0.108 \quad (7)$$

$$C_{Dw} = 20(M_\infty - M_{crit})^4 \quad (8)$$

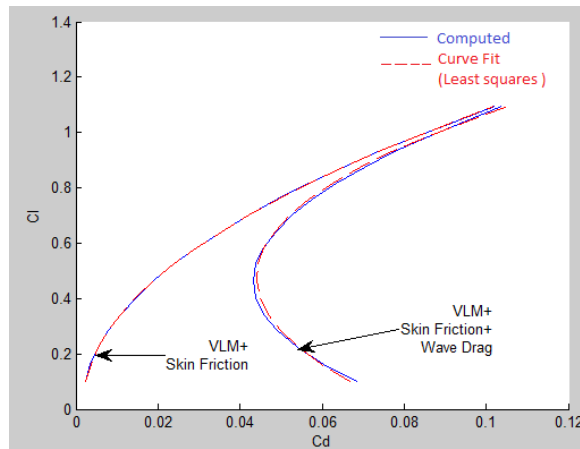


Fig. 4 – Drag Polar

### 2.3 Mass Estimation

Generally mass estimation methods can be categorized into finite element, empirical and the semi-empirical approach. Finite element is known to provide reliable estimates but would increase computational cost in the initial design phases. On the other hand, empirical methods combine aircraft parameters and statistically derived coefficients but are of low fidelity [10]. Semi-empirical methods hence provide a suitable balance needed for the conceptual design of unconventional configurations. An approach of combining semi-empirical methods for essential components and empirical methods for others is used to maintain fidelity and save computational costs. Care is taken to estimate the bulk of the mass such as airframe and systems using class II methods. As the airframe is the main component that is unconventional applying such techniques would suffice. Other components those are mostly conventional in the nature of their design and requirement for the aircraft can be estimated by regular methods as there is not much deviation from general aviation requirements. The Howe airframe mass prediction is based on the models provided by the Howe's Algorithm. The structural mass of a conventional aircraft comprises the mass of fuselage, wing, control surfaces and the empennage. For a BWB, however, the structural mass is idealized to the mass of the outer and inner wings (Fig. 5) corrected for deviations from the ideal mass [11]. The mass of the wing can be given as:

$$M_{wing} = M_c + M_r + f_{pen} \quad (9)$$

Thus, breaking down the equation first the mass of the covers are computed,

$$M_c = \frac{n_{ult} \times MTOM \times b^3 \times r \times e \times \sec(\Lambda_{c/4}) \times \sec(\Lambda_{c/2})^{0.5} \times \rho \times C_r^{0.25} \times 10^{-5}}{A \times t/c} \quad (10)$$

Then the mass of the ribs is computed,

$$M_r = 4.4 \times S_{ref} \times e \times (C_r \times t/c)^{0.5} \times \left(1 + 0.35 \times \frac{\Lambda_c}{2} \times \rho \times 10^{-3}\right) \quad (11)$$

Finally, the penalty factor is estimated,

$$f_{pen} = 0.1 \times MTOM \times \left(\frac{S_{fin}}{S_{refout}}\right) \quad (12)$$

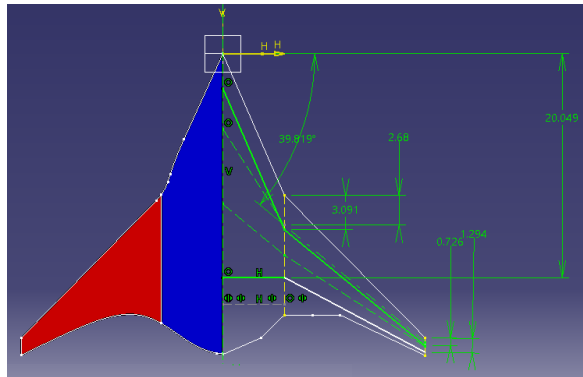


Fig. 5 – Idealized Wing (Inner: Blue Outer: Red)

Following results plotted in Fig. 6 are obtained on running the Mass module code developed in MATLAB. Convergence is obtained after 10 iterations. Initial weight estimation shows promising results. About 18.8 % Reduction in MTOM. However this is without any constrains with regard to specified mission requirements.

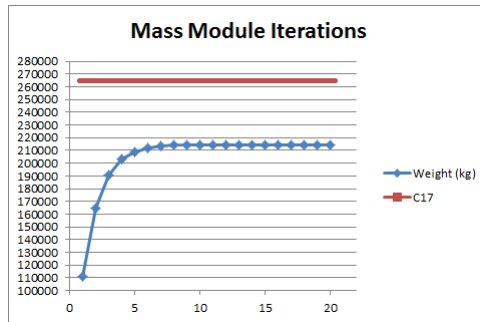


Fig. 6 – Mass Module (X axis: Iterations; Y axis: Weight (kg))

### 2.4 Constraint Analysis

In order to establish a design space with regard to the required mission profile the relationship between two most important controlling parameters namely Thrust to weight ratio (T/W) and Wing loading (W/S) is to be determined by subjecting them to mission requirement constrains. The general master equation derived from the free-body analysis is used for the computations,

$$\frac{T_{SL}}{W_{TO}} = \frac{\beta}{\alpha} \left\{ \frac{qS}{\beta W_{TO}} \left[ K_1 \left( \frac{n\beta W_{TO}}{qS} \right)^2 + K_2 \left( \frac{n\beta W_{TO}}{qS} \right) + C_{Do} + C_{DR} \right] + \frac{P_S}{V} \right\} \quad (13)$$

The keys to the development of these relationships, and a typical step in any design process, are reasonable assumptions for the aircraft lift-drag polar and the lapse of the engine thrust with flight altitude and Mach number. It is not necessary that these assumptions be exact, but greater accuracy reduces the need for iteration. It is possible to satisfy these aircraft/engine system requirements as long as the thrust loading at least equals the largest value found at the selected wing loading [12].

The T/W as a function of W/S is needed for the following:

- 1) Takeoff from a runway of given length;
- 2) Flight at a given altitude and required speed;

- 3) Turn at a given altitude, speed, and required rate;
- 4) Landing without reverse thrust on a runway of given length.

What is important to realize is that any combination of T/W and W/S that falls in the “solution space” automatically meets all of the constraints considered. For better or for worse, there are many acceptable solutions available at this point and it is important to identify which is “best” and why [12]. The obtained design space for the baseline-1 configuration is shown in Fig. 7.

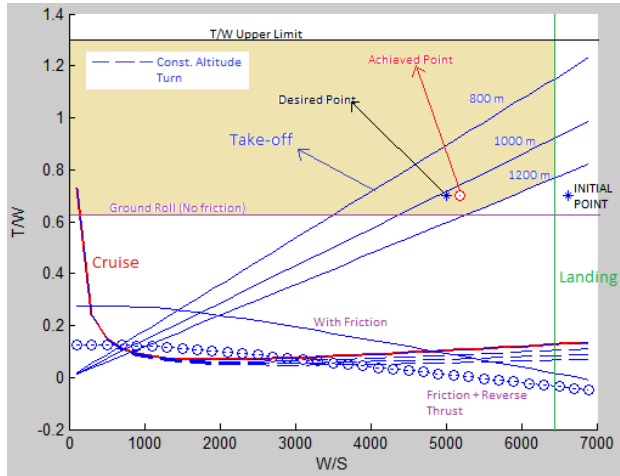


Fig. 7 – Constraint analysis (Yellow region: Design space of Baseline-2)

## 2.5 Modifications in the Computational Module

The computational module developed during the baseline-2 design is modified to take in the new modifying parameters due to the adapter fuselage. An inverse design block is introduced in the preliminary aerodynamics module to analyze and develop new resulting airfoils satisfying the locus criterion. The new structure requires rerunning the entire algorithm subject to the new geometric design, airfoil stack and weight. The mass module iterations are optimized to keep the entire MOTM lower than that of the C17 as a design requirement. The developed constrain analysis module makes sure all optimizations result in realistic results within the required design space. This is also required to incorporate inherent stability as required by the second primary objective. Hence a static and dynamic sub-module constitutes this block which optimizes for static and dynamic stability requirements. A more detailed explanation of this sub-module can be found later in section four.

## 3. THE HYBRID “ADAPTER” FUSELAGE

In order to support conventional military operations a cargo inlet bay with a cylindrical configuration is required in a cargo aircraft. The main challenge will be to parametrize the resulting complex geometry formed by blending a cylindrical fuselage with the baseline-2 design. This will also result in the change in the root airfoil shape hence a loss of lift can be expected. The design effort would be to reduce loss of lift as much as possible so as to avoid making the blended wing redundant. Previously proposed by Lockheed Martin a simple approach of just blending a conventional adapter fuselage to the rear end of a BWB design sounds simple and effective. However it can be said that a loss in lift would be imminent. Moreover difficulty in manufacturing and parametrizing the resulting complex geometry is

expected. A reflex airfoil is characterized by an upward cusp in the trailing edge. This is akin to the raised cylindrical fuselages often needed in cargo airplanes (Fig. 8). This approach proposes to therefore use reflex airfoils to develop the adapter fuselage section for the cargo compartment. It is hoped that this will allow for the decrease in lift required for the elliptical lift profile and also satisfy the cargo inlet cabin constrains. Therefore thickness and trailing edge cusps of the reflex airfoils from the finalized baseline-2 design are increased in order to fit the required inlet area. The new airfoil stack is now updated for beginning iterations in the developed computational module.



Fig. 8 – Comparison of C17 fuselage shape with scaled reflex airfoil

However in the first step that is the preliminary aerodynamics module the optimized lift distribution is not satisfactory and overall lift coefficient drop to a very low value of 0.0421. The only explanation seems to be that there is considerable negative lift being generated due to the scaled and modified reflexed airfoils. Therefore in order to address this issue two steps are proposed:

1) Increase of wing area

The previous designs were developed by keeping certain constrain from the C-17 however their objective was to develop and demonstrate the superiority of the BWB configuration. Now that it is established certain constrains can be relaxed to as to achieve design objectives as in this case an increase in wing area is required. However care is taken so as to not surpass the total MTOM of the C-17. This is simply done with the motive of designing a lighter yet efficient competitor. The aerodynamic module is invoked and utilized for optimization so as to arrive at a total wing area that satisfies the said objectives and still keeps the aircraft in the required design space.

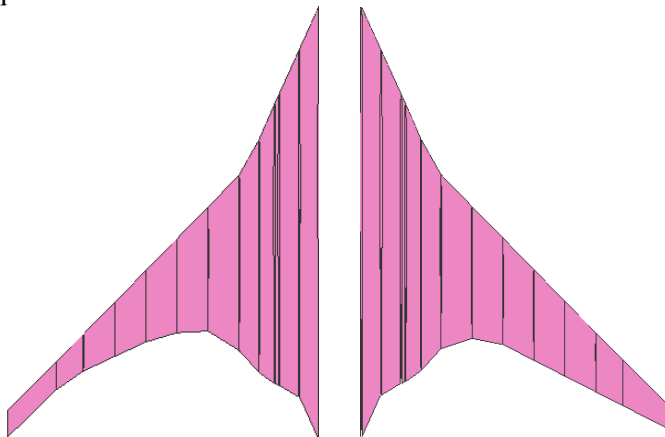


Fig. 9 – Comparison of wing planform (Baseline 2 –left & Baseline 3 –right)



The trailing edge of the baseline 2 design is increased so as to do away the curvature and make the outer wing a trapezoidal configuration. Fig. 9 shows the comparison for the old and new wings. Slight differences are introduced in the inner wing so as to maintain curve smoothness at the kink station where the inner and outer wings meet.

## 2) Development of a new approach

A new approach of ‘Hybrid airfoil shape fitting is proposed for the adapter fuselage. Here the design geometric development would be in a similar approach to how the baseline-2 design was parametrized.

The new approach proposes to:

- a. To fit trailing edge points of several thick airfoils in the locus of the cylinder.
- b. To arrange the airfoil stack in a conic fashion utilizing the “lifting fuselage concept”.

In essence the cylindrical fuselage is cut into several discs each having a unique diameter. The root airfoil surface are arranged such that they meet at the three dimensional locus formed by the respective circles. Hence by controlling the equations of the circles it now becomes possible to control the shape of the morphed structure. An extrapolated and simple form is shown in the Fig. 10. In actuality the step size between the circles and airfoil stacks is very small to get a smooth three dimensional locus.

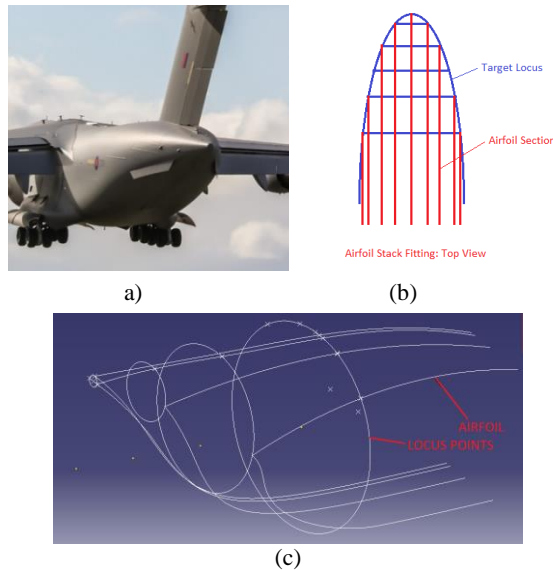


Fig. 10 – Hybrid airfoil fitting in 3D locus: (a) Cargo bay of C-17; (b) A schematic example of airfoil stack fitting; (c) 3D locus along with airfoil fit

Possible advantages include maintenance of required shape and cargo bay inlet area and lift contribution by the structure. The new approach promises to make the design stay true to the BWB principle i.e. an entire lifting surface.

Moreover it allows the rear complex geometry to be parametrize making it reproducible in algebraic form or in CAD. Fitting airfoils in the new locus requires modification of the original airfoil coordinates.

Hence optimization is imperative to maintain fidelity. Although slight loss of lift is imperative due to this modification of the airfoil shape however optimization is done to reduce this.

Moreover the arrangement done in conic sections utilizing the lifting body concept helps in developing an entire lifting structure.

#### 4. STABILITY CHARACTERIZATION

In order to design inherent stability this sub-module is introduced to compute resulting stability parameters and enable stability constrained optimization. Initial conditions required for both static and dynamic stability are introduced. These results are further used to design the horizontal and vertical stabilizers. An important point to note is that the adapter fuselage also allows for easy integration of an empennage which is an added advantage. To design inherent static stability the computation module is related to the mass and aerodynamic modules as shown in Fig. 11 and iterated for two necessary conditions:

1. Negative slope of moment coefficient vs angle of attack curve with positive y intercept.
2. Negative static margin.

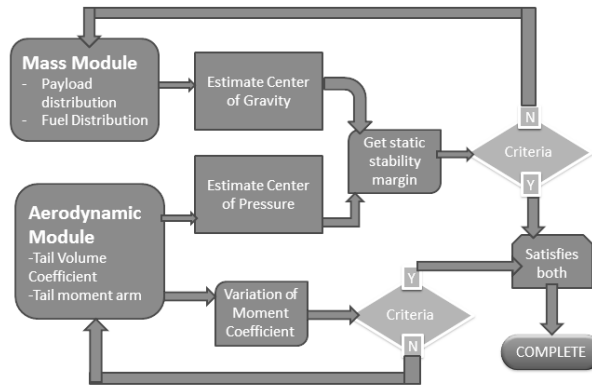


Fig. 11 – Stability Analysis Module

The variables to optimize are the payload distribution and the location of the empennage that is the tail moment arm. The payload distribution can be safely assumed to lie exactly under or above the center of gravity. The center of pressure is estimated using results from the aerodynamic module and center of gravity is calculated using results from the mass module and a force balance method. The moment arm is varied and using resulting tail volume coefficient the smallest possible empennage is designed satisfying the two mentioned criteria. The center of mass of the airframe is computed in XFLR5. From the mass estimation module mass of the power plants, payload, empennage and fuel distribution is derived. Finally a force balance method is used to compensate for the additional components to the initial estimate from XFLR5.

$$C_{M_{cg}} = C_{M_{ac}} + C_L \left[ \frac{x_{cg} - x_{ac}}{c} \right] + C_{M_{FN}} - \eta_t V_H C_{L_t} \quad (14)$$

$$V_H = \frac{S_t l_t}{S_w c} \quad (15)$$

$$\eta_t = \frac{V_t^2}{V_\infty^2} \quad (16)$$

(Total Mass) x **c.g** =

$$\begin{aligned} & (\text{Dry mass of body only}) \times (\text{c.g of body}) + (\text{fuel mass}) \times (\text{c.g of fuel}) + (\text{mass} \\ & \text{of first 2 engines}) \times (\text{c.g of first 2 engines}) + (\text{mass of other 2 engines}) \times (\text{c.g of} \\ & \text{other 2 engines}) + (\text{mass of empennage}) \times (\text{c.g of empennage}) \end{aligned} \quad (17)$$

Dynamic stability of aircraft refers to the response and performance of aircraft to perturbations over time.

Along with designing inherent static stability it is imperative to introduce dynamic stability as well.

The dynamic stability can be characterized in the frequency domain by transforming the flight model equations.

The resulting Eigen values from the solved state matrix is used to derive information about the dynamic characteristics of the aircraft. This analysis is done to establish the natural longitudinal and directional response of the aircraft in order to establish the requirements of control, handling and stability augmentation.

A well-defined aircraft will have 2 symmetric phugoid modes, 2 symmetric short period modes, 1 spiral mode, 1 roll damping mode and 2 Dutch roll modes [13]. The VLM model developed in XFLR5 is used for initial analysis.

Further detailed dynamic stability models can be later implemented for characterization of control and handling qualities.

For now the VLM model is used to directly derive all stability derivatives and compute the state matrix.

The control matrix is neglected as only the natural modal response is desired for now. Calculation of the Eigen modes is done by using the state-space variable representation of equations of motion.

Root locus and modal response is then determined. The state-space representation is given by,

$$\dot{x} = Ax + BI \quad (18)$$

where A is the stability matrix and B is the control matrix.

$$A = \begin{bmatrix} X_u & X_w & 0 & -g \\ Z_u & Z_w & u_0 & 0 \\ M_u + M_w Z_u & M_w + M_w Z_w & M_q + M_w U_0 & 0 \\ 0 & 0 & 1 & 0 \end{bmatrix} \quad (19)$$

X,Z and M are the stability derivatives computed from the VLM model. This matrix is computed and solved for

$$|A - \delta I| = 0 \quad (20)$$

The solution gives the Eigen values representing the various dynamic modes of the aircraft.

## 5. RESULTS AND DISCUSSIONS

### 1. Hybrid airfoil shape fitting:

New airfoils are developed for each section using a supercritical base airfoil by inverse design methods and fitted according to the required locus by varying chord and trailing edge shape. Hence a perfectly morphed fuselage shape is obtained (Fig. 12) which while maintaining compatibility still provides lift.

The new hybrid fuselage solves the compatibility issue as it provides the same circular area as in a conventional cargo inlet bay and simultaneously is also a lifting structure.

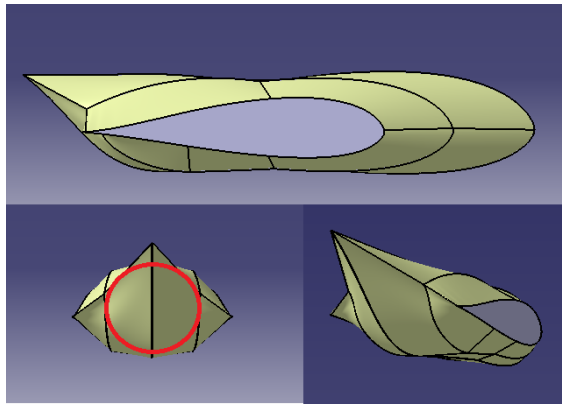


Fig. 12 – Final adapter fuselage design  
(Red circle represents minimum required & equivalent C17 inlet bay area)

2. Span wise lift distribution:

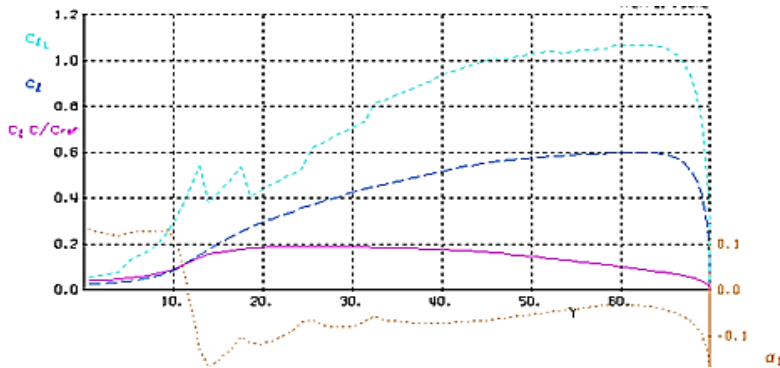


Fig. 13 – AVL Trefftz Plane showing final lift distribution

The overall lift coefficient (Fig. 13) reduced from **0.28** to **0.248** as a consequence of the adapter fuselage but is still close to the Boeing design BWB having a  $C_L$  of **0.25**. Therefore it can be said that the designed fuselage achieves the objective of ensuring compatibility while not incurring significant lift penalty.

What is also favorable is that the local coefficients do not cross the 0.6 limit at the wing tips which otherwise would produce huge magnitudes of wave drags as estimated by previous studies [14].

3. Mass Estimation:

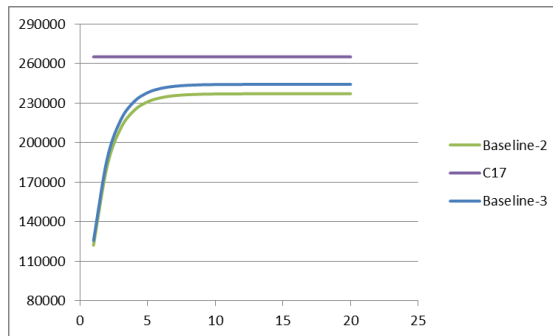


Fig. 14 – Mass Module (X axis: Iterations; Y axis: Weight (kg))

As expected the adapter fuselage ended up contributing slightly to the overall mass as shown in Fig. 14. The new MTOM = 244180 kg is however still lesser than that of the C-17. This result is essentially important since it portrays the flexibility inherent in a pure blended wing body configuration.

Despite incorporating several modifications care was taken while optimization to keep the final MTOM constrained with a magnitude below than that of the C-17.

#### 4. Constraint Analysis:

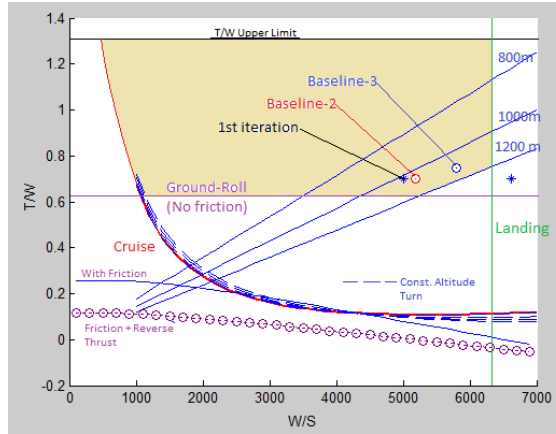


Fig. 15 – Constraint Analysis (All design points)

Rerunning the constraint analysis module gave the new design point although comparing figure 15 with 7 show hardly any difference in the design space. The deviation from baseline-2 to baseline-3 is due to increase in weight and increase in wing area. However the final point is inside the favourable design space. The take-off distance is between 1000m to 1200m. Although the current configuration is fixed for now there is still space for modifications such as an increase in wing span to reduce the take-off distance.

#### 5. Final Baseline-3 Parameters:

Table 1 – Final parameters and percentage change for Baseline-3 from C17

Parameter	Unit	C-17	Baseline -2	Baseline -3	Change (From C17)
W/S	N/m <sup>2</sup>	7362	4980	5796	21.27 % (↓)
T/W	-	0.69	0.772	0.7495	8.62 % (↑)
Wing Area	m <sup>2</sup>	353.11	466.98	413.3	17 % (↑)
Wing Span	m	51.75	36	42.672	17.54 % (↓)
MTOM	kg	265000	237030	244180	7.85 % (↓)
Payload Mass	kg	77500	82000	82000	5.5 % (↑)
Range (Berguet)	km	7200	10553	11553	60.46 % (↑)

A summary of important parameters are given in table 1. The most important results are the reduction in MTOM and increase in range. The MTOM decreases by about 7.8% which is consistent with previous predictions of around 11% decrease for a pure BWB design. The slight variation may be attributed to the hybrid adapter fuselage. The large increase in range may be explained by the fact that the Baseline -3 range has been estimated by the Berguet Range equation while the specified C-17 range is the official value as stated in the company website. It may be argued that there might be slight variation between the actual and Berguet estimations. However given the fact of a higher L/D ratio and cruise velocity of the

baseline-3 a higher range may be safely expected. The current design also has a shorter wingspan than the C-17 hence there are still enough margins if further improvement in lift, range or any other performance parameter is required.

6. Stability:

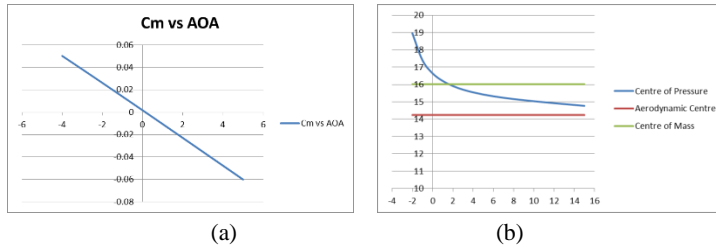


Fig. 16 – (a) Moment Coefficient variation with angle of attack; (b) Variation of center of mass, aerodynamic center and center of pressure with angle of attack

The variation obtained satisfies the set criterion of a negative slop and positive intercepts (Fig. 16). The intercepts however are very small. This can be attributed to the fact that the empennage designed to overcome the pitching moment of the wing was designed with the criteria of being as small as possible and the moment arm being not longer than the root chord. The location of the center of mass is ahead of the center pressure for angles upto two degrees however above it the center of pressure moves ahead of the center of mass. Hence a negative static margin is maintained up to two degrees of angles of attack only. At this stage this is an undesirable effect and hence hints at the need for a stability augmentation system.

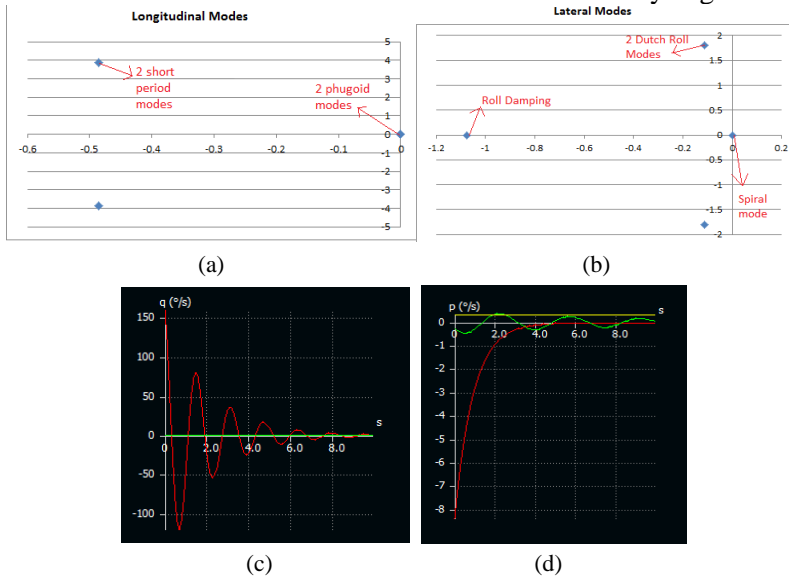


Fig. 17 – (a) Longitudinal Modes; (b) Lateral Modes; (c) Pitch rate modal response; (d) Roll rate modal response

All modes are in the left half plane indicating stability due to damping (Fig. 17). It is important to note that the Phugoid modes are very close to Imaginary axis. Roll damping is non-oscillatory. Spiral mode is also non-oscillatory but in positive half plane indicating instability. Using the developed VLM model in xflr5 a modal response for the obtained Eigen values is plotted to deduce the nature of the natural frequencies of the design. The pitch rate and yaw rate modal variation is consistent with the interpretations from the root locus. Although the rates attain equilibrium the response time is not as good as standalone

BWB designs [15]. Hence there is a requirement of better control characterization along with a need of a stability augmentation system.

#### 7. CAD Prototype:

Many geometric tolerances, intricate surface contours and defects can be identified and corrected using CAD software. For realizing the baseline-3 design CATIA V5 software is used owing to its extensive use in the aerospace industry and user friendly techniques available for aircraft design. The finalized model developed in CATIA is exported to Autodesk Fusion 360 for final rendering shown in Fig. 18. The CAD model is also developed to serve as the input geometry for a computational fluid dynamics analysis.

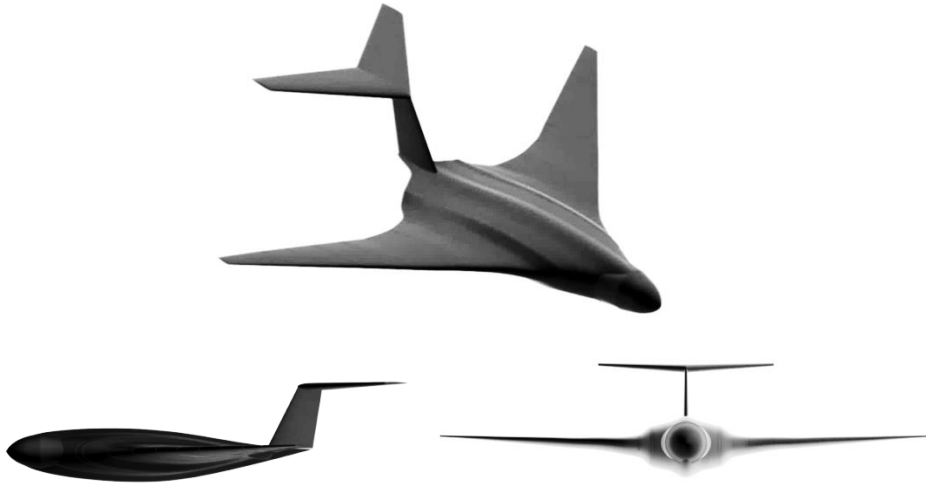


Fig. 18 – Three views of the final rendered model

## 6. CONCLUSIONS AND FUTURE WORK

The aerodynamic and stability characterization for the design of a next generation cargo aircraft was proposed. A novel approach of a hybrid adapter fuselage body was taken to simultaneously solve the said compatibility issue and ensure no lift loss. A robust analysis technique for the unconventional design was developed constituted by combinations of empirical and semi-empirical or class II methods. The design effort was constrained within real world mission profile requirements to quantitatively establish the superiority of the proposed configuration. Finally a CAD prototype was developed for further study and validation. Current and Future work:

- In order to obtain more data points and to ensure further validation and optimization Euler based computational fluid dynamic analysis is in progress promising to further reduce drag by at most 55% [16].
- To further enhance stability and fine tune handling characteristics a control characterization and development of some autopilot or stability augmentation system is required.
- Experimentation work aimed at validating some but important parameters are also needed to further support the claims made. This may range from wind tunnel testing to flight tests of a scaled prototype.
- A feasibility study for incorporating turboelectric propulsion is proposed as a future objective to improve efficiency.

## REFERENCES

- [1] T. Eric, A. Joel, P. Ishaan, C. Nhat, *Blended Wing Body (BWB) Aerodynamic Analysis and Redesign*, 16.100 Undergraduate Project Report, Massachusetts Institute of Technology, Cambridge, Massachusetts, USA, December 2015.
- [2] R. Liebeck, Design of the Blended Wing Body Subsonic Transport, *Journal of Aircraft*, Vol. **41**, pp. 10–25, 2004.
- [3] J. L. Felder, H. D. Kim, G. V. Brown, *Turboelectric Distributed Propulsion Engine Cycle Analysis for Hybrid-Wing-Body Aircraft*, 47<sup>th</sup> AIAA Aerospace Sciences meeting, AIAA-2009-1132, 5-8 January 2009, Orlando, Florida, USA.
- [4] P. Ishaan, K. Shruthi, G. Deepak, *Aerodynamic Analysis and Redesign of Blended wing Body*, Undergraduate Thesis, SRM University, Kattankulathur, India, May 2016.
- [5] \* \* \* *Lockheed Martin Refines Hybrid Wing-Body Airlifter Concept*, Aviation Week & Space Technology, Feb 17, 2014. Available Online: <http://aviationweek.com/awin/lockheed-martin-refines-hybrid-wing-body-airlifter-concept> (accessed on 2/11/2016).
- [6] J. Fuchte, T. Pfeiffer, P. D. Ciampa, B. Nagel, V. Gollnick, *Optimization of Revenue Space of a Blended Wing Body*, 29<sup>th</sup> Congress of the International Council of the Aeronautical Sciences, St. Petersburg, Russia, 7-12 September 2014, Vol. **1-6**, pp. 361-370.
- [7] \* \* \* Boeing, *C 17 Globemaster Technical Specifications*. Available online: <http://www.boeing.com/defense/c-17-globemaster-iii/#/facts> (accessed on 5/12/2016).
- [8] M. Drela, *AVL User guide*. MIT Aero & Astro. Available online: [http://web.mit.edu/drela/Public/web/avl/avl\\_doc.txt](http://web.mit.edu/drela/Public/web/avl/avl_doc.txt) (accessed on 11/12/2016).
- [9] J. I. Hileman, Z. S. Spakovszky, M. Drela, M. A. Sargeant, Airframe Design for “Silent Aircraft”, *Journal of Aircraft*, Vol. **47**, No. 3, pp. 956-959, 2010.
- [10] P. P. C. Okonkwo, *Conceptual Design Methodology for Blended Wing Body Aircraft*, PhD Thesis, Cranfield University, UK, May 19, 2016.
- [11] D. Howe, Blended Wing Body Airframe Mass Prediction, *Journal of Aerospace Engineering*, Proceedings of the Institution of Mechanical Engineers, Part G:, pp. 319–331, 2001.
- [12] S. A. Brandt, R. J. Stiles, J. J. Bertin, R. Whitford, *Introduction to Aeronautics: A Design Perspective*, 2<sup>nd</sup> ed.; AIAA, Virginia, USA, pp. 19-54, 2004.
- [13] R. C. Nelson, *Flight Stability and Automatic Control*, 2<sup>nd</sup> ed.; McGraw-Hill Ryerson, Limited, USA, pp. 34-111, 1998.
- [14] N. Qin, A. Vavalle, A. L. Moigne, Spanwise lift distribution for blended wing body aircraft, *Journal of Aircraft*, Vol. **42**, pp. 356- 365, 2005.
- [15] P. Sanjiv, R. Shailendra, G. Saugat, K. S. Kshitiz, B. Sudip, Aerodynamic and Stability Analysis of Blended Wing Body Aircraft, *International Journal of Mechanical Engineering and Applications*, Vol. **4**, No. 4, pp. 143-151, doi: 10.11648/j.ijmea.20160404.122016.
- [16] A. R. Thomas, W. Z. David, *Aerodynamic Shape Optimization of a Blended-Wing-Body Regional Transport for a Short Range Mission*. 31<sup>st</sup> AIAA Applied Aerodynamics Conference June 24-27, 2013, San Diego, CA. (DOI: 10.2514/6.2013-2414).